UNIVERSIDADE DE SÃO PAULO

INSTITUTO DE FÍSICA
CAIXA POSTAL 66318
05389-970 SÃO PAULO - SP
BRASIL

PUBLICAÇÕES

IFUSP/P-1165

MEASUREMENTS OF TEMPERATURE FLUCTUATIONS AND PLASMA EDGE TURBULENCE IN THE TBR-1 TOKAMAK

R.M. Castro, M.V.A.P. Heller, I.L. Caldas, R.P. da Silva, Z.A. Brasilio, I.C. Nascimento
Instituto de Física, Universidade de São Paulo

Junho/1995

Measurements of temperature fluctuations and plasma edge turbulence in the TBR-1 tokamak

R.M. Castro, M.V.A.P. Heller, I.L. Caldas, R.P da Silva, Z.A. Brasilio,

I.C. Nascimento.

Institute of Physics, University of São Paulo

C.P.66318, 05389-970 São Paulo, SP, Brazil

To investigate the tokamak turbulence, a set of Langmuir probes and a triple probe have been designed and used in the TBR-1 to measure average and fluctuating values of density, potential, and temperature of the plasma edge. The obtained results show that there is a significant influence of the temperature fluctuations in the transport parameters. Namely, taking into account this influence, the density and plasma potential power spectra have been obtained, and the turbulence parameters reevaluated. Furthermore, the computed cross power-spectra show appreciable linear correlation, and the cross-bispectra show a quadratic mode coupling between temperature fluctuations and other quantities.

PACS Numbers: 5235R, 5270.

I. Introduction

The interest in the study of plasma edge is based on the evidence that the properties of the plasma confinement depend on the edge behavior.[1,2] The temperature, potential, and density fluctuation levels, their phases, and coherences can provide information about the basic mechanisms determining edge turbulence.[3,4] Particularly, these measurements are necessary for a complete estimation of particle and energy transport in this turbulent plasma.[5,6]

However, despite the intensified studies of plasma transport in toroidal plasmas over the past ten years, there are still few measurements of temperature fluctuations and their correlations with other fluctuating quantities.[7–15] This lack of results is expected, since the temperature fluctuations have the same frequencies as density and potential fluctuations and usually it is technically difficult to make accurate temperature measurements, and obtain conclusive interpretations, using Langmuir probes at frequencies higher than 100 kHz

Despite these technical difficulties, some interesting results have already been obtained by using swept probe[7,11,13,16] and triple probe techniques.[8,9,10] Although the swept probe technique has the advantage of measuring oscillations at only one space position, there are hardware limitations, due to sweeping speed, and doubts about the correct fitting of the probe characteristic curves ($I \times V$). On the other hand, the triple probe measures directly the temperature fluctuations, but uses signals from two space positions. These results indicate that temperature fluctuations should not be neglected to estimate several relevant turbulence characteristics in tokamaks and

stellerators, as density and plasma potential fluctuations, fluctuation induced energy and particle transport.

In this paper we report measurements of plasma-edge parameters (density, potential, and electron temperature) obtained by using a specially designed system of Langmuir probes.[17] Besides a common single probe and four single probes configured in a square array (to measure floating potential and ion saturation current fluctuations), this probe system contains also a modified triple-probe used to measure the (average and fluctuating) electron temperature.[8,9,18] Thus, it is possible to measure simultaneously the temperature fluctuations and the mentioned mean parameters and other fluctuating quantities. Furthermore, we also use advanced digital signal analysis techniques, including a bispectral estimation method, to reduce the obtained data and determine any possible correlation involving temperature fluctuations and other quantities.

This investigation indicates that at the TBR-1 plasma edge the relative levels for temperature fluctuation, about 15%, have the same order of magnitude than those obtained for the density and fluctuating potential; therefore, they must be taken into account in order to correctly estimate the plasma edge turbulence. Moreover, their observed linear and quadratic correlations indicate their importance to interpret the plasma edge turbulence. Thus, knowing the corrected edge parameters, we compare the experimental conclusions with those predicted by turbulence drift wave theories.[1–3,5,6]

The remaining sections of this paper are organized as follows: section II is a description of the experiment, section III presents the results, namely, the corrected frequency spectra and radial profiles, and discussion, and section IV gives the conclusions.

II. Description of the experiment

The experiment was carried out on the Ohmically heated TBR-1 tokamak with major radius $R = 0.30$ m, minor radius $a = 0.08$ m, toroidal magnetic field $B_\phi = 0.4$ T, plasma current $I_p \simeq 10$ kA, chord average density $n_o \simeq 1 \times 10^{19}$ m^{-3}, and pulse length of $\simeq 10$ ms.[20] The plasma in the TBR-1 has a circular cross section and a full poloidal limiter at one toroidal location. The vessel was conditioned with Taylor discharge cleaning method, and the gas used was hydrogen. For results presented in this paper, the toroidal field was in the same direction of the plasma current.

The data were collected from a multipin Langmuir probe, Fig. 1, inserted into the plasma through a diagnostic port located on the top of the tokamak, 45° toroidally displaced from the poloidal limiter. This multipin tungsten probe could be moved radially between shots. The collecting part of these probes was 2 mm long and 0.75 mm in diameter. This probe system was composed by a square array of four tips (3 mm × 3 mm), a four-pin probe array and a single probe tip. Typically, two of the square array tips measure the floating potential fluctuations, $\tilde{\varphi}_f$, and the other two measure the ion saturation current fluctuations, $\tilde{I}_{si}$. These two pairs of pins were used for determining the spectrum $S(k, f)$ and power weighted average values of poloidal wave vector, k_θ, frequency, f, phase velocity, v_{ph}, and width of the k_θ.[21] The single tip, at 3 mm from the square matrix, was used to directly measure the mean value of

floating potential, φ_f.

Electron mean temperature, T_e, its fluctuation, $\tilde{T}_e$, ion saturation current, I_{si}, and its fluctuation, $\tilde{I}_{si}$, were obtained using a modified triple probe technique[8,9,18,22] with four pins for phase delay error corrections. This error arose from finite probe tip separation across field lines. The probes were carefully adjusted to minimize shielding effects and gain differences.

The probe measurements were performed during the flat top phase of the plasma current, in time intervals of approximately 4 ms and averaged over seven consecutive shots. The time series measurements were recorded using 8 bit digitizers, with a maximum sampling rate of 1 MHz. The length of the used data consisted of 105 samples of 256 points. These series were submitted to a statistical criterion to eliminate spurious points which otherwise would contribute to an overestimation of fluctuations.

Temperature from the triple probe was given by:

$$KT_e = e(V_+ - V)/ln2 \,, \tag{1}$$

where V was the mean of two floating potentials (measured symmetrically to V_+) and V_+ was the potential of the positively biased probe.[18] The plasma density was obtained by:

$$n \,\alpha\, I_{si}/T_e^{1/2} \,. \tag{2}$$

The quantities measured with the triple probe were decomposed, using a numerical filter, into mean ($f < 5$ kHz) and fluctuating ($5 < f < 500$ kHz) parts.

Density and potential fluctuations corrected by temperature fluctuations were obtained by:[8,9,18]

$$\tilde{n} = n\left[\frac{\tilde{I}_{si}}{I_{si}} - \frac{1}{2}\frac{\tilde{T}_e}{T_e} + \frac{1}{4}\left(\frac{\tilde{T}_e}{T_e}\right)^2\right] \tag{3}$$

and

$$\tilde{\varphi}_p = \tilde{\varphi}_f + \frac{\sigma K\tilde{T}_e}{e} \,, \tag{4}$$

where σ is considered equal to 2.8. The plasma potential (φ_p) is related to the floating potential (φ_f) through an equation similar to equation (4). The relative level profiles of the fluctuating parameters, $\tilde{\alpha}$, were given by the root-mean-square, α^{rms}, defined as:

$$\alpha^{rms} = <(\tilde{\alpha} - \alpha)^2>^{1/2} \,, \tag{5}$$

where α is the mean value of the parameter.

The observed level of temperature fluctuations in the edge means that corrections to the ion saturation current and floating potential measurements are needed to yield more reliable information about density and plasma potential fluctuations.

III. Results and Discussion

Radial profiles of the mean density, potential, and electron temperature are plotted in Fig. 2. As it can be seen from this figure, the edge density and temperature are in the range: $n \simeq (0.2-9.0)\times 10^{17}$ m^{-3} and $T_e \simeq (6-35)$ eV. In addition, in the radial interval $0.9 < r/a < 1.1$, the density scale length is $L_n \simeq 0.6\times 10^{-2}$ m, whereas

the temperature scale length is $L_{Te} \simeq 1.0 \times 10^{-2}$ m.

The uncertainty in the estimation of plasma potential, from the probe floating potential, is substantial because the exact value of σ in Eq. (4) is difficult to determine.[1] In the plasma edge the plasma potential decreases outwards. From the φ_p radial profile the mean radial electric field is estimated to be $E_r \simeq 16 \times 10^2$ V/m in the limiter shadow and $E_r \simeq 35 \times 10^2$ V/m in the plasma edge. This last value of radial electric field is comparable to the one that would be created by stochastic magnetic field lines, according to Ref. 23:

$$E_r \simeq T_e[L_n^{-1} + 0.5L_{Te}^{-1}] \simeq 36 \times 10^2 \text{ V/m} . \quad (6)$$

The radial profile of the root-mean-square of the temperature fluctuation is shown in Fig. 3a. The influence of the corrections introduced by temperature fluctuations, according Eqs. 3 and 4, on the potential and density fluctuation profiles are shown in Figs. 3b and 3c. At some radial positions the corrected values are at least 30% higher than those obtained neglecting the mentioned corrections. As it was reported in References 8, 9, 10, and 16, these fluctuation levels introduce significant errors in the turbulence description if they are not taken into account in the Eqs. (3) and (4). Indeed, these corrections are remarkably important in the plasma edge, although they can not also be neglected even in the scrape-off-layer. Thus, the observed temperature fluctuations affect significantly the previous interpretations of probe data in the TBR-1.[24,25]

To determine if the fluctuations are due to a density gradient drive, we also plotted

in Fig. 3d the radial variation predicted for drift waves:[6,19]

$$\frac{e\tilde{\varphi}_p}{KT_e} \simeq \frac{\tilde{n}}{n} \simeq 4\rho_s/L_n , \quad (7)$$

where ρ_s is the Larmor radius (estimated by assuming $T_i \simeq T_e$) and L_n is the density scale length. In Eq. 7 the use of the factor 4 encloses the prediction of both the Waltz-Dominguez and Terry-Diamond models.[19] As we can see, even the corrected experimental profiles are incompatible with the model prediction.

In Fig. 3d, we also plotted the fluctuation radial profile calculated for the self-sustaining drift wave model according to the following expressions:[5,26]

$$\tilde{n}/n \;\alpha\; (L_s^2 n Z)^{1/2} B_\phi^{-1/2} T_e^{-3/4} L_{Te}^{-3/2} \quad (8)$$

and

$$\frac{e\tilde{\varphi}_p}{KT_e} \;\alpha\; (L_s^2 n Z)^{1/2} B_\phi^{-1/2} T_e^{-3/4} L_{Te}^{-3/2} , \quad (9)$$

where the magnetic shear is given by:

$$L_s = q^2 R_o/aq' , \quad (10)$$

q is the safety factor and Z is the effective charge state. Since L_s and Z were not directly available, we used their mean values over the observed radial range. For the fluctuating potential, the computed radial profile (Fig. 3d) is consistent with the measured one (Fig. 3b), although the computed and the measured magnitudes are

different. Moreover, this model predicts neither the profile nor the magnitude of the fluctuating density. However, as predicted from this model, our results show that:

$$\frac{e\tilde{\varphi}_p}{KT_e} > \tilde{n}/n \ . \tag{11}$$

The relative magnitude of the temperature fluctuations were $T_e^{rms}/T_e \simeq 0.15$. For these values, the computation of the potential and density profiles at plasma edge are considerably affected.

Fig. 4 shows the frequency power spectra of temperature fluctuations computed from data measured at the radial position $r/a = 0.81$ and $r/a = 0.96$. At the plasma edge the temperature fluctuation spectra are similar to those obtained for the other fluctuations.

A two point estimate of the $S(k, f)$ spectrum[21] indicates that both the waves vector poloidal component, k_θ, and its spectral width, $\sigma_{k\theta}$, are reduced if they are computed with temperature corrections. This effect is observed in Figs. 5a and 5b where we see the $S(k, f)$ spectrum, for fluctuating potential at $r/a = 0.81$, computed without and with temperature fluctuation corrections. The poloidal wave number spectrum narrows with correction.

Fig. 6 shows the frequency spectra of the fluctuation driven particle flux at $r/a = 0.96$ considering and neglecting the correction introduced by the temperature fluctuations. The driven particle flux spectrum is calculated by:[19]

$$\Gamma = 2\, k_\theta\, |P_{\tilde{n}\,\tilde{\varphi}}|\, \sin(\theta_{\tilde{n}\,\tilde{\varphi}})/B_\phi \ . \tag{12}$$

Besides the influence of temperature fluctuations in the particle flux, Fig. 6 shows also the fact that the flux is mostly supported by low frequency components. As it can be seen, in this case the corrections affected not only the intensity of the fluctuations but also the direction of their poloidal propagation. Consequently, near the limiter the integrated transport was higher than the computed incorrected value.

In order to determine a possible relationship between the measured fluctuations, the cross-spectra of fluctuations were computed. We observed that the ion saturation current and floating potential fluctuations are in phase and present a linear coherence $\gamma \simeq 0.5$ at frequencies below 100 kHz. In the frequency range for which the coherence is above the noise level, the linear coherence between floating potential fluctuations and temperature fluctuations is lower than coherence between ion saturation current and temperature fluctuations (Fig. 7). As observed in other machines,[14] the phase calculation between ion saturation current and temperature fluctuations shows that they are almost in antiphase for frequency components until 100 kHz. To investigate the coupling between the measured fluctuations, we used a bispectral analysis technique.[27–29] In the present analysis the recorded data are not enough to neglect the variance of bicoherence. However, since the bicoherence is larger than $1/\mathrm{M} \cong 0.0047$ (where $M = 210$ is the number of successive realizations with time intervals of 128 μs), we can still consider the coupling of the modes using bispectral analysis. By inspection of the autobicoherence of floating potential, ion saturation current and temperature fluctuations, we concluded that non linear interactions are concentrated mainly at $10 \leq f_2 \leq 50$ kHz and $25 \leq f_1 \leq 60$ kHz and have significant level

only for temperature fluctuations.

Fig. 8a shows the integrated bicoherences, $\sum b^2$, for fluctuating temperature and potential at $r/a = 0.81$; where b^2 is the bicoherence corresponding to a triplet f_1, f_2 and $f = f_1 + f_2$. Each value of $\sum b^2$ is a sum of b^2 for all f_1 and f_2 satisfying the resonant condition $f = f_1 + f_2$ within the spectral region $0 \leq f_2 \leq f_N/2$ and $f_2 \leq f_1 \leq f_N - f_2$, where f_N is the Nyquist frequency. As it is shown in Fig. 8a, the nonlinear coupling is negligible for the potential fluctuations. However, for temperature fluctuations the sum of bicoherence is close to unity possibly indicating the presence of coherent structures. The bicoherence of fluctuating temperature and plasma potential show similar behavior for all radial positions in the plasma edge; however, near the limiter and in the SOL these computed bicoherences are negligible.

Fig. 8b shows the bicoherence of potential and temperature fluctuations at $r/a = 0.81$ for interactions satisfying the resonant condition $f = f_1 + f_2$, with f fixed at $\simeq$ 35 kHz. In the case of the two considered fluctuations for the same resonant condition we do not see any contribution from modes of the high frequency band. In the case of cross-bicoherence between temperature, ion saturation current, and floating potential, the quadratic coupling is more significant for the first two fluctuations. Accordingly, Fig. 8c shows the cross-bicoherence between temperature and ion saturation current at $r/a = 0.92$ with values of $\sum b_c^2 \cong 0.4$.

Calculated values of skewness and kurtosis for the measured fluctuations are very near the expected values for Gaussian distributed signals, so probability distribution functions for the analysed data, indicate no significative deviation from normal

distribution.

IV. Conclusions

In the TBR-1 tokamak, a complex system of Langmuir probes was used at the edge to determine plasma parameters, namely, temperature, density and plasma potential, as well their broadband fluctuations. Besides a square array of four single probes, to measure the fluctuation spectra, and one single probe to measure the plasma potential, a modified triple probe was used to measure the mean and fluctuating temperatures. Accurate tests were exhaustively done to assure the reliability of those obtained data, specially in the case of the not so common triple probe. Thus, it was possible to obtain the corrected levels of the electrostatic fluctuation intensities, taking into account the temperature fluctuations, in order to obtain the right radial profiles of the measured quantities and to perform the spectral and bispectral analyses of the obtained data.

Radial profiles of n, φ_p and T_e were determined. At the plasma edge these radial profiles are well approximated by exponentials with scale lengths $L_n \simeq 0.6 \times 10^{-2}$ m and $L_{Te} \simeq 1.0 \times 10^{-2}$ m. This n profile steepness was also observed in other tokamaks as COMPASS and START.[16]

The resultant broad-band power spectra for the fluctuating density, floating potential, and temperature are similar, suggesting a common driving source for these turbulent fluctuations. However, as reported before,[10] differences in the slope of these fluctuations were observed above 100 kHz. These differences may be relevant to identify near-Gaussian probability distribution functions[30,31] and to distinguish structures in the turbulent fluxes at the plasma edge.[32]

The corrections due to the measured temperature fluctuations introduced significative alterations in the magnitude of the relative values $\tilde{n}/n$ and $e\tilde{\varphi}_p$ / KT_e. However, the radial profiles of these quantities are not modified by these corrections. Therefore, we must use the corrected parameters to check the theoretical predictions.

Thus, for the plasma edge, the drift wave scaling[6] $\simeq 4\rho_s/L_n$ still fails to predict the radial dependence for $e\tilde{\varphi}_p$ / KT_e and $\tilde{n}/n$. With respect to the behavior predicted by the self-sustaining drift waves model, [19,26] only the inequality $e\tilde{\varphi}_p$ / $KT_e > \tilde{n}/n$ and the $e\tilde{\varphi}_p$ / KT_e profile were verified.

In the region accessible to the probes, the frequency spectrum of temperature fluctuations is similar to the density and fluctuating potential spectra. From the $S(k,f)$ spectra we conclude that the spectral width σ_k is reduced and the σ_f is increased with temperature corrections.

The ion saturation current and temperature fluctuations were strongly correlated, while the fluctuations of temperature and fluctuating potential were only weakly correlated. The phase calculation between $\tilde{T}_e$ and $\tilde{I}_{si}$ showed that they were almost in antiphase for frequency components below 100 kHz.

The reported analysis showed that neglecting $\tilde{T}_e$ in the turbulent particle flux calculation altered significantly the results in the plasma edge. In fact, the previous fluxes, for radial positions near the limiter, were computed without taking into account the observed strong increase in the phase difference between $\tilde{n}$ and $\tilde{\varphi}_p$, $\theta_{\tilde{n},\tilde{\varphi}}$ (see Eq. 11).

The nonlinear coupling calculated through the integrated bicoherence of temper-

ature fluctuations was not negligible, specially for low frequency modes with high power. Cross bicoherence between $\tilde{I}_{si}$ and $\tilde{T}_e$ was more significant than that between $\tilde{\varphi}_f$ and $\tilde{T}_e$.

Finally, probability distribution functions of these fluctuations indicate no significant deviations from normal distribution.

Acknowledgments

The authors would like to thank Dr. Roger D. Bengtson (Fusion Research Center, The University of Texas at Austin) for his useful suggestions, E. Sanada, A.P. dos Reis, F.T. de Gasperi for technical support and Dr. A.N. Fagundes and W.P. de Sá for computational assistance. This research was sponsored in part by FAPESP and CNPq.

[1]A.J. Wootton, B.A. Carreras, H. Matsumoto, K. McGuire, W.A. Peebles, Ch. Ritz, P.W. Terry, S.J. Zweben, Phys. Fluids **B2**, 2879 (1990).

[2]F. Wagner, U. Stroh, Plasma Phys. Control. Fusion **35**, 1321 (1993).

[3]D. Biskamp, *Nonlinear Magnetohydrodynamics*, Cambridge University Press, Cambridge (1993).

[4]S.J. Camargo, *Lectures Notes on Turbulence in Fluids and Plasmas*, Institute of Physics, University of São Paulo, Report IFUSP/P-1148 (1995). S.J. Camargo, H. Tasso, Phys. Fluids **B4**, 1199 (1992).

[5]J.D. Callen, Phys. Fluids **B4**, 2142 (1992).

[6]W. Horton, Phys. Rep. **192**, 1 (1990).

[7]P. Liewer, C.M. McChesney, S.J. Zweben, R.M. Gould, Phys. Fluids **29**, 309 (1986).

[8]H. Ji, H. Toyama, K. Yamagishi, S. Shinohara, A. Fujisawa, K. Miyamoto, Rev. Sci. Instrum. **62**, 2326 (1991).

[9]H. Ji, H. Toyama, K. Miyamoto, S. Shinohara, A. Fujisawa, Phys. Rev. Lett. **67**, 62 (1991).

[10]H. Lin, G.X. Li, R.D. Bengtson, Ch.P. Ritz, H.Y.W. Tsui, Rev. Sci. Instrum. **63**, 4611 (1992).

[11]A. Carlson, L. Giannone, ASDEX Team, *Proceedings of the 18th European Conference on Controlled Fusion and Plasma Physics.* (Berlin, 1991), **IV**, 305 (1991).

[12]Lin, R.D. Bengtson, Ch.P. Ritz, Phys. Fluids **B1**, 2027 (1989).

[13]R. Balbin, C. Hidalgo, M.A. Pedrosa, I. García-Cortés, J. Vega, Rev. Sci. Instrum. **63**, 4605 (1992).

[14]C. Hidalgo, R. Balbin, M.A. Pedrosa, I. García-Cortés, M.A. Ochando. Phys. Rev. Lett. **69**, 1205 (1992).

[15]S. Sattler, H.J. Hartfuss and the W7-AS Team, *Proceedings of the 21th European Conference on Controlled Fusion and Plasma Physics* (Montpellier, 1994), **III**, 1220 (1994).

[16]J.G. Ferreira, *Electrostatic Probe Measurements on Tokamak Plasmas*, Ph.D. thesis, Department of Engineering Science, University of Oxford (1995).

[17]R.M. Castro, M.V.A.P. Heller, Z.A. Brasilio, I.L. Caldas, R.P. da Silva, I.C. Nascimento,*Proceedings of the 1994 International Conference on Plasma Physics* (Fóz do Iguaçu, 1994), INPE-IUPAP, **1**, 381 (1994).

[18]H.Y. Tsui, R.D. Bengtson, G.X. Li, H. Lin, M. Meier, Ch.P. Ritz, A.J. Wootton, Rev. Sci. Instrum. **63**, 4608 (1992).

[19]T.L. Rhodes, C.P. Ritz, R.D. Bengtson, Nucl. Fusion **33**, 1147,(1993).

[20]I.C. Nascimento, I.L. Caldas, R.M.O. Galvão, J. Fusion Energy 12, 529 (1993).

[21]S.J. Levinson, J.M. Beall, E.J. Powers, R.D. Bengtson, Nucl. Fusion **24**, 527 (1984).

[22]S.L. Chen, T. Sekiguchi, J. Appl.Phys, **36**, 2363 (1965).

[23]R.W. Harvey, M.G. McCoy, J.Y. Hsu, A.A. Mirin, Phys. Rev. Lett. **47**, 102 (1981).

[24]R.M. Castro, M.V.A.P. Heller, I.L. Caldas, R.P. da Silva, Z.A. Brasilio, Il Nuovo Cimento **15D**, 983 (1993).

[25]M.V.A.P. Heller, R.M. Castro, I.L. Caldas, Z.A. Brasilio, R.P. da Silva, Nucl. Fusion, **35**, 59 (1995).

[26]B. Scott, Phys. Rev. Lett. **65**, 3289 (1990).

[27]T. Estrada, E. Sanchez, C. Hidalgo, B. Brañas, Ch. P. Ritz, *Proceedings of the 20th EPS Conference on Plasma Physics and Controlled Fusion* (Lisboa, 1993), **I**, 373 (1993).

[28]K. Rypdal, F. Øynes, Phys. Lett.A **184**, 114 (1993).

[29]H.Y.W. Tsui, K. Rypdal, Ch.P. Ritz, A.J. Wootton, Phys. Rev. Lett. **70**, 2565 (1993).

[30]R. Jha, P.K. Kaw, S.K. Mattoo, C.V.S. Rao, Y.C. Saxena, R. Singh, ADITYA Team, Nucl. Fusion **33**, 1201 (1993).

[31]A.V. Filippas, R.D. Bengtson, G.X. Li, M. Meier, Ch.P. Ritz, E.J. Powers, *Conditional Analysis of Floating Potential Fluctuations at the Edge of the Texas Exper-*

imental Tokamak Upgrade (TEXT-U), Fusion Research Center, The University of Texas, Report FRCR #453 (1994).

[32]L. Kadanoff, *Scaling and Multiscaling (Fractals and multifractals), in Nonlinear Phenomena in Fluids, Solids, and Other Complex Systems*, edited by P. Cordero and B. Nachtergaele, Elsevier Science Publishers B.V., 456 (1991).

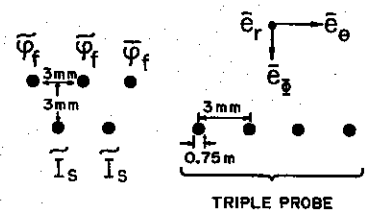

Fig. 1 - Scheme of probe system.

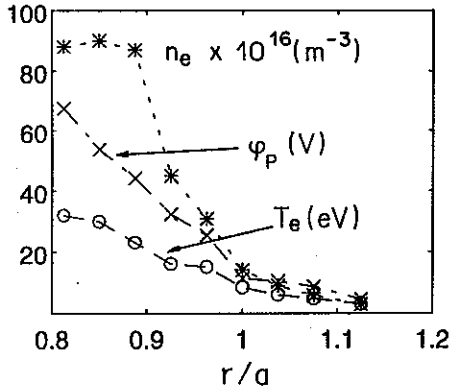

Fig. 2 - Edge plasma profiles for density, potential and temperature.

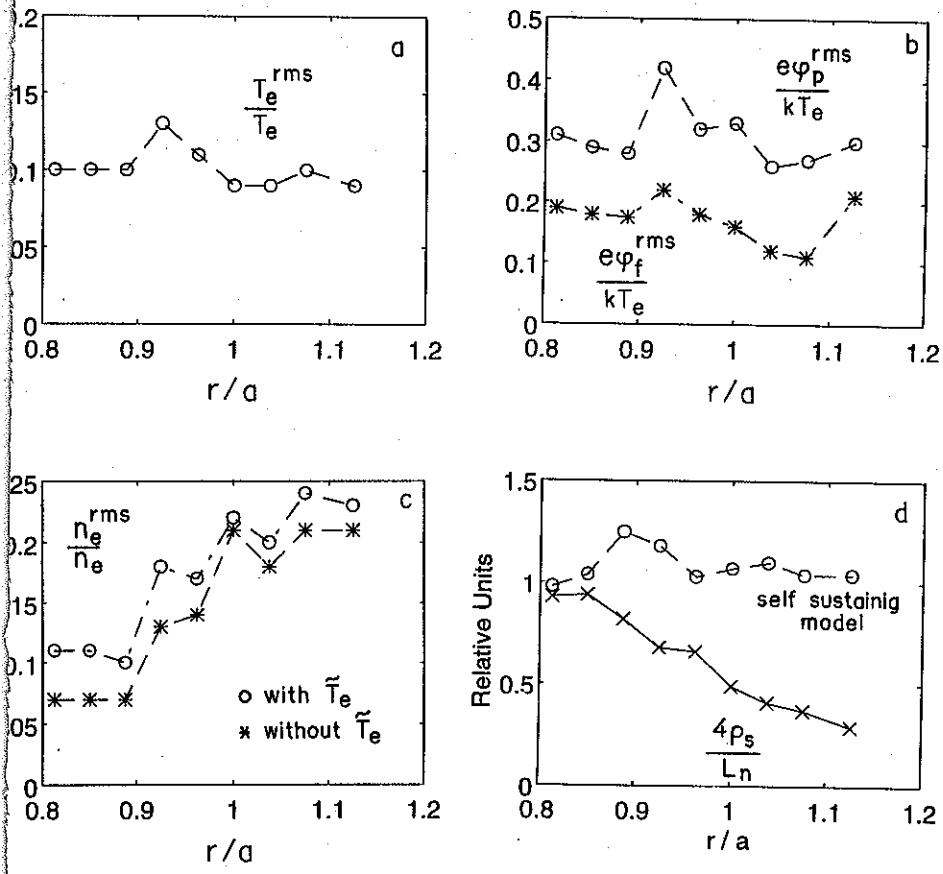

Fig. 3 - Relative root-mean-square (rms) profiles for temperature fluctuations (a), floating potential (b), and density (c), (neglecting (*) and considering (o) the temperature fluctuations). Relative profiles for two theoretical models (d).

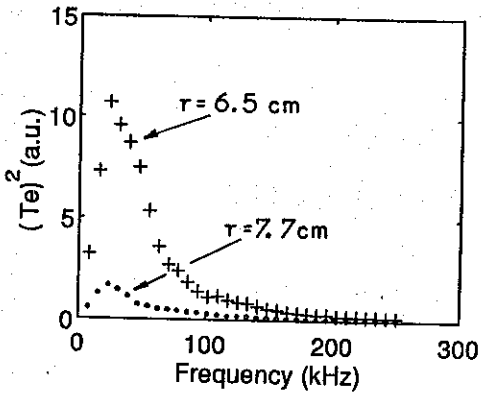

Fig. 4 - Power-spectra of temperature fluctuations at two radial positions, at $r/a = 0.81$ (+) and at $r/a = 0.96$ (o).

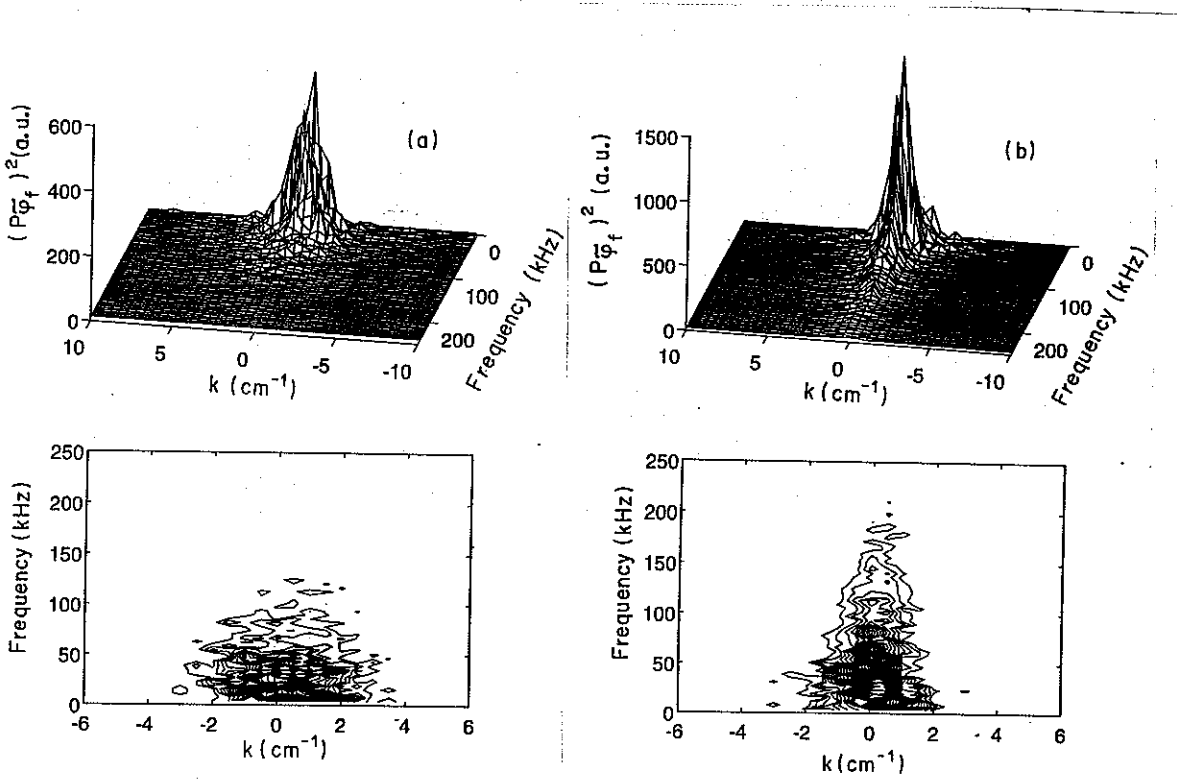

Fig. 5 - $S(k, f)$ spectra and contours at $r/a = 0.81$, without temperature corrections (a), and with temperature corrections (b).

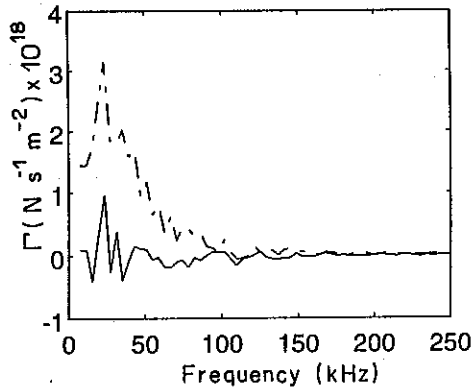

Fig. 6 - Induced particle flux spectra at $r/a = 0.96$, with temperature fluctuations correction (dashed curve) and without correction (full curve).

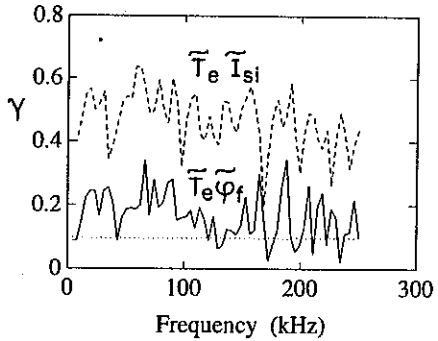

Fig. 7 - Coherence at $r/a = 0.92$ of $\tilde{T}_e$ with $\tilde{I}_{si}$ and $\tilde{\varphi}_f$ (dashed and full curves respectively). Straight line denotes statistical uncertainty.

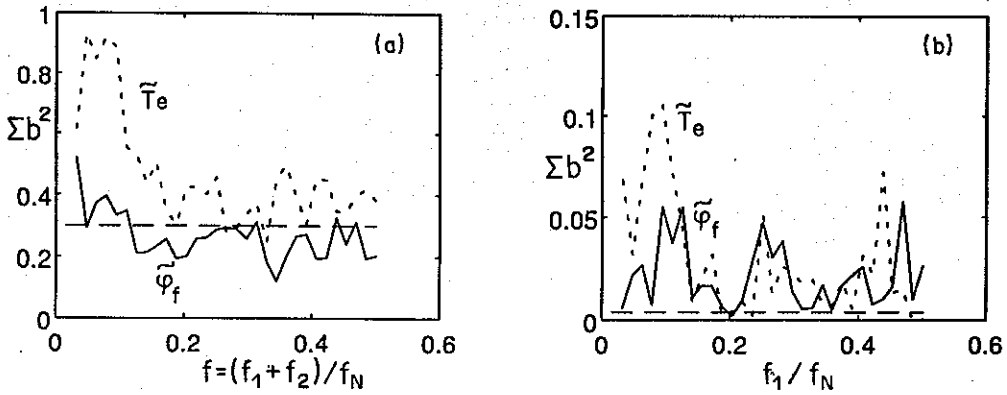

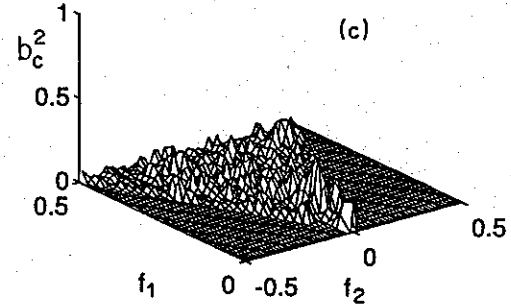

Fig. 8 - At $r/a = 0.81$, integrated bicoherence for $\tilde{T}_e$ (dashed curve) and $\tilde{\varphi}_f$ (full curve) (a). Bicoherence for the same parameters for interactions satisfying the resonant condition $f = 35$ kHz (b); straight line denotes statistical uncertainty. Cross bicoherence between $\tilde{T}_e$ and $\tilde{I}_{si}$, at $r/a = 0.92$ (c). Frequencies normalized to Nyquist frequency and filtered at 250 kHz.